Remote Sensing of Environment 278 (2022) 113084

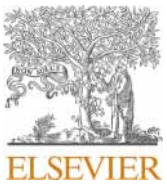

Contents lists available at ScienceDirect

Remote Sensing of Environment

journal homepage: www.elsevier.com/locate/rse

The new era of regional coastal bathymetry from space: A showcase for West Africa using optical Sentinel-2 imagery

Christopher Daly [a,*], Wassim Baba [b], Erwin Bergsma [c], Gregoire Thoumyre [a], Rafael Almar [a], Thierry Garlan [d]

[a] LEGOS/IRD, UMR-5566, 14 Avenue Edouard Belin, 31400 Toulouse, France
[b] LEGOS/CNRS, UMR-5566, 14 Avenue Edouard Belin, 31400 Toulouse, France
[c] Earth Observation Lab, CNES, 18 Avenue Edouard Belin, 31400 Toulouse, France
[d] SHOM, 13 rue du Chatellier, 29200 Brest, France

ARTICLE INFO

Edited by Menghua Wang

Keywords:
Optical imagery
Waves
West Africa
Underwater features
Satellite-derived bathymetry

ABSTRACT

Large-scale coastal bathymetry is paramount to understand natural and human-induced coastal behaviour and plays a vital role in coastal research and governance. Here, we use a recently developed algorithm, S2Shores (Satellite to Shores), to invert coastal bathymetry from wave kinematics, based on the linear dispersion relation. Wave numbers and celerity are extracted from optical Sentinel-2 imagery, by exploiting the small temporal offset between the image bands of its Multi-Spectral Instrument. Inverted depths are output at 200 m resolution, and individual depth points are merged to create a composite bathymetry using a weighted average of images from 10 different dates. The resulting bathymetry mosaic spans 4000 km along the West African coast. S2Shores is able to detect depths up to 35 m, depending on mean incident wave conditions and cloud cover, which varies by location. Underwater features are well reproduced by S2Shores, such as flow channels in Guinea, the St. Ann's Shoal in Sierra Leone, and ebb delta lobes at several outlets along the Niger River Delta. S2Shores results match well (r^2 = 0.76, RMSE = 4.9 m) with a bathymetry survey along the Senegalese coast. As a difference with traditional satellite-derived bathymetry methods based on water colour, a wave-based approach allows estimations in turbid areas and relatively deep waters, which suggest that the two approaches are complementary and should be used in combination to cover coastal environments in their diversity. The new possibility offered by this regional coastal atlas opens the door to increased research and planning capabilities and sets an example that can be applied to the rest of the world.

1. Introduction

Accurate, highly resolved coastal bathymetry is a vital dataset heavily needed in science, industry, governance, and military applications, as the change of bathymetry provides fundamental understanding of the natural behaviour of coastlines and the impacts of engineering projects, and it serves as a boundary condition for numerical studies (Cesbron et al., 2021). Traditionally, acoustic (single-track and multi-beam echo sounders) methods have been used to collect bathymetry data; but even with the best efforts, it is not cost-effective for mapping coastal areas on a regional or even global scale, as only 18% of the world's oceans and 50% of coastal areas have been surveyed at 1-min (1.852 km) resolution (Becker et al., 2009; GEBCO Compilation Group, 2019). As such, the hydrographic community has turned to remote sensing techniques to help fill gaps between sparse records of acoustically-measured depths. The General Bathymetric Chart of the Oceans (GEBCO, GEBCO Compilation Group (2019)), one of few publicly available global bathymetry datasets, is created by using the gravity anomaly from satellite altimetry data, which is related to variations in-depth, to interpolate depths between in-situ soundings (Smith and Sandwell, 1997, 2004). As most soundings are located in deep oceanic waters, coastal areas (< 100 m depth) are often poorly resolved, especially where there are abrupt changes in the shelf-slope, resulting in unrealistic representation of shallow features such as deltas and atolls. The quality of GEBCO depth estimates is also limited by the sparsity of its source data, especially in data-poor regions such as West Africa.

* Corresponding author.
E-mail address: dalyjchris@gmail.com (C. Daly).

https://doi.org/10.1016/j.rse.2022.113084
Received 3 May 2021; Received in revised form 27 April 2022; Accepted 13 May 2022
Available online 3 June 2022

Coastal bathymetric surveys in this area are 30 years old on average (as shown in GEBCO metadata[1]). The lack of detailed coastal bathymetric data leads to unacceptable uncertainties in coastal wave and flood models, in subsequent risk assessments and forecasts, and currently limits the best coastal management strategies for the region (Ndour et al., 2018).

Additional methods of direct depth measurement using Earth Observation remote sensing techniques are therefore needed to produce large-scale (i.e. regional to global) bathymetries (Benveniste et al., 2019; Melet et al., 2020; Salameh et al., 2019; Almar et al., 2021b; Cesbron et al., 2021). This may be achieved using aircraft and satellite laser (LiDAR) (Saylam et al., 2018; Abdallah et al., 2013; Parrish et al., 2019; Thomas et al., 2021) or satellite-derived bathymetry (SDB), either using radar (Stewart et al., 2016; Bian et al., 2020) or optical missions. For the latter, the two most advanced techniques which allow direct measurement of depth by satellite are water colour (Stumpf et al., 2003; Lyzenga et al., 2006; Lee et al., 2010; Hodúl et al., 2018) and wave kinematics (Poupardin et al., 2016; Danilo and Melgani, 2016; Almar et al., 2019a; Bergsma et al., 2019b). SDB methods which rely on colour and light absorption as a proxy from which to estimate depth are limited to shallow water with on average maximum detectable depths of approximately 15 m (Pacheco et al., 2015; Chénier et al., 2018; Traganos et al., 2018). These methods are sensitive to local environmental conditions which affect water clarity, such as turbidity and bottom vegetation, and light absorption in the atmosphere. Methods using wave kinematics, on the other hand, exploit timing differences between a sequence of satellite images (or image bands) of the sea surface taken in rapid succession to detect the movement of surface waves. For example, satellite images from the Pleiades satellite mission (Airbus/CNES) can collect a burst of up to 12 very high-resolution (0.5 m) images timed 8 s apart Almar et al. (2019a), while the Multi-Spectral Instrument (MSI) of the Sentinel-2 mission (ESA), collects surface reflectance data with a maximum 1.005 s interval between 10 m resolution bands. Various analytic techniques can then be used to extract wave celerity data from the image sequences, either in the temporal (Almar et al., 2019a) or spectral-domain (Bergsma et al., 2019a, 2021).

At regional to global scale, new LiDAR for bathymetry from IceSat-2 Parrish et al. (2019); Thomas et al. (2021) but also colour-based methods in optical for there high resolution and also radar missions (like Sentinel-1) for cloudy environments seem very promising. With the advantages and disadvantages of each method/technology, the future lies in merging the estimates into a combined composite Earth observations approach. For example, IceSat2 bathymetry or the colour-based method that are more likely to be obstructed by turbidity can be used to calibrate/validate the wave-based method or used in combination or sequentially as the applicability is exactly complementary: wave/non-wave moments.

Here, we use a recently developed method for estimating coastal bathymetry using multiple (at least two) optical images (Bergsma et al., 2019a, 2019b, 2021), in this case two Sentinel-2 colour-bands. The method, called Satellite to Shores (hereafter S2Shores), exploits the time difference between the blue and red bands (2 frames taken 1.005 s apart) to track the movement of surface waves over time and space. A novel localized Radon Transform combined with a Discrete fast Fourier Transform (DFT) technique is used to determine the dominant wave direction and corresponding wavelength and celerity at the peak image intensity. Water depths can then be inverted using the linear dispersion relationship. Using wave kinematics as input allows maximum depths up to 100 m to be detected (theoretically) under optimal wave conditions (i.e. long swell) (Bergsma and Almar, 2020). This technique can therefore be used to estimate the depth in most coastal environments exposed to waves without dependence on water clarity or atmospheric light absorption, with depth outputs at resolutions up to 50 m. The method relies on the presence of waves which occurs worldwide along the coasts, with different frequency and characteristics (Bergsma and Almar, 2020).

Here we present the first regional SDB atlas along the West African coast (West Coast and Gulf of Guinea, from Senegal to Gabon). In this region, 253,970 km^2 of the continental shelf lies within a depth range of 0–100 m (coastal zone), based on GEBCO data. Of this coastal zone, 18% (70,700 km^2) lies between 0 and 15 m depth — the theoretical sensing range of most colour-based methods, which may be even less after accounting for water quality along coastal West Africa. On the other hand, 70% (178,060 km^2) of the target area lies between 2 and 50 m depth — the average sensing range of most wave-based methods for this region (Bergsma and Almar, 2020). As this article follows from the work of Bergsma et al. (2019a, 2019b) and Baba et al. (2021) with further development of the S2Shores algorithm and its numerical implementation, this work primarily details a methodology for pre-selection and post-processing of Sentinel-2 imagery in order to produce depth composites.

2. Area of interest

The area of interest (AoI) spans the coastal area of West Africa and the Gulf of Guinea between Senegal and Gabon (Fig. 1). This 4000 km length of coastline, covered by 73 Sentinel-2 tiles, consists of a wide range of coastal features and types, including long sandy beaches, barrier islands, rocky capes, offshore islands, estuaries, and deltas. The width of the shallow coastal zone in the AoI varies considerably. It is widest ($<$ 25 km) in the deltaic region spanning the Gambia, Guinea-Bissau, Guinea and Sierra Leone (the Guinea Terrace) (McMaster et al., 1970; Anthony, 2004), and along the Niger Delta. It is mildly sloping in Senegal (10–20 km wide), the Bight of Benin and Bonny, and most narrow ($>$ 5 km) along the coast of Liberia, immediately north of Dakar and around Bioko Island, Equatorial Guinea.

The West African coast from Senegal to Liberia generally faces westerly Atlantic swells, while Ivory Coast to Nigeria is exposed to south Atlantic swells (Almar et al., 2019b). Cameroon to Gabon, in the Bight of Bonny (Biafra), is relatively sheltered by offshore islands (e.g. Bioko, Equatorial Guinea). Seasonality in wave conditions is observed along the entire West African coast. The Volta and Niger rivers produce the two largest deltas along the coast. Sediment supply from these deltas is constantly moved alongshore by long swell waves which drive persistent eastward longshore transport between Ghana and Nigeria (Anthony et al., 2016; Almar et al., 2015; Giardino et al., 2018). As such, these areas are susceptible to ongoing erosion at the western side and accretion at the east (Dada et al., 2016; Anthony et al., 2019).

Mean cloud cover varies over the AoI, with occasional cloud cover at Senegal (coastal area in close proximity to the Sahara Desert), with $<$ 20% coverage 50% of the time, and increasingly persistent cloud cover further south in tropical equatorial regions, especially in the Bight of Bonny, with up to $<$ 80% coverage 50% of the time (Bergsma and Almar, 2020).

3. Data and methods

Three main steps are followed in the production of depth estimates at a particular Sentinel-2 tile location: 1) pre-selection of images from the Sentinel-2 database, 2) running the S2Shores algorithm for each image, and 3) post-processing of raw depths in order to minimise errors and produce a final depth composite. In minimizing errors, GEBCO data is used as a first-order proxy for depth at the scale of the image tile. These steps, shown schematically in Fig. 2, are explained in detail in the following sub-sections.

[1] https://maps.ngdc.noaa.gov/viewers/iho_dcdb

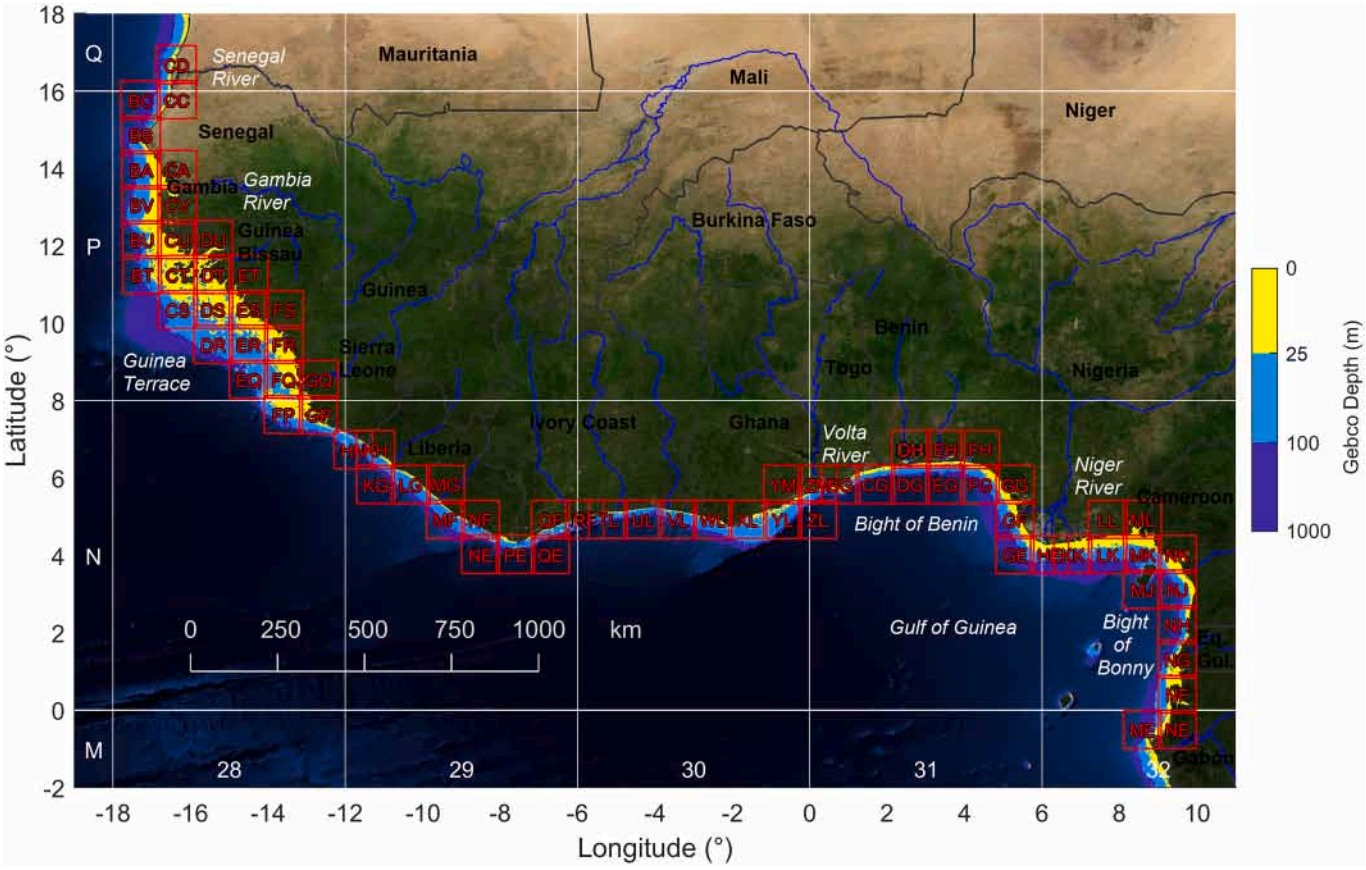

Fig. 1. Area of interest in West Africa and Gulf of Guinea, from Senegal in the north to Gabon in the south. GEBCO bathymetry contours shown at 0, 25, 100 and 1000 m depths. The 73 red squares show the group of Sentinel 2 coastal tiles making up the study area, along 4000 km of coastline. Each tile is 109×109 km. The name of each tile is constructed by using the UTM zone corresponding to the coordinates of its lower left corner as a prefix (UTM zone grid shown in white) and a sub-UTM zone identifier as a suffix (shown at the center of each square, in red). For example, 28PBB is the tile where Dakar, Senegal (the westernmost point in Africa) is located. *Background image: MODIS Blue Marble, NASA Earth Observatory.* (For interpretation of the references to colour in this figure legend, the reader is referred to the web version of this article.)

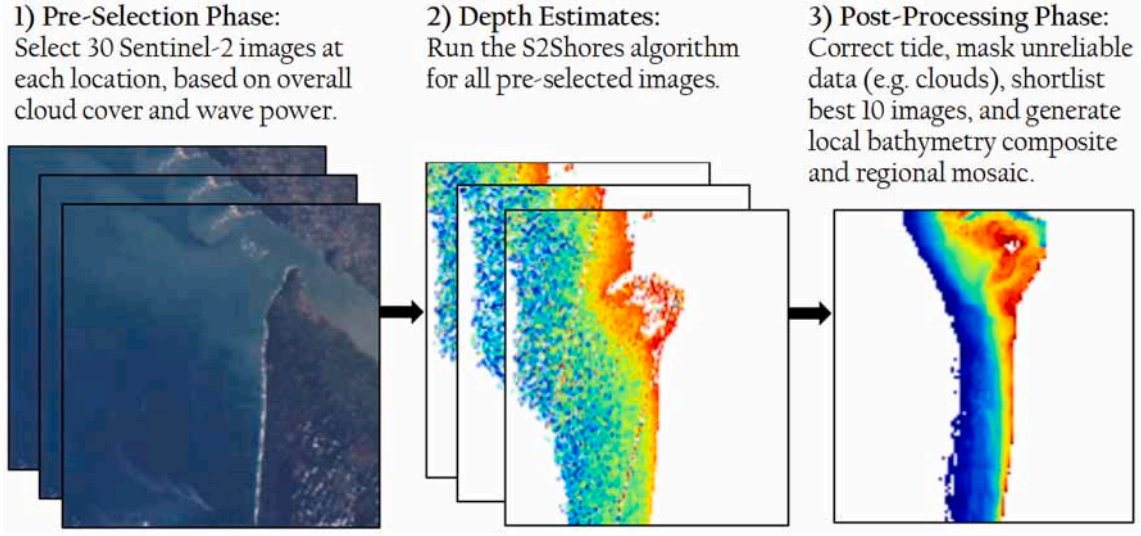

Fig. 2. An overview of the methodology for the derivation of bathymetry composites at Sentinel-2 tile locations.

3.1. Pre-selection of Sentinel-2 images

The recently launched Copernicus Sentinel-2 Mission[2] captures multi-spectral satellite image data at least every 5 days at the equator. There are therefore approximately 6 images per month at a particular location which may potentially be used for depth estimation. Each Sentinel-2 satellite image has 13 spectral bands with a footprint of 109.8×109.8 km. Of the 13 spectral bands, four are sampled at 10-m resolution, of which three represent visible colours blue, green and red (bands 2–3-4, respectively), while band 8 represents the near-infrared (NIR) part of the electromagnetic spectrum. Data from bands 2 and 4 are used in the S2Shores algorithm Bergsma et al. (2019a).

The Sentinel-2 image database currently spans a period of 6 years from 2015 to present, resulting in at least 250 images per tile (single orbit). With such a large number of observations, a global analysis including all images will be inefficient and time consuming. We therefore pre-select the best images for analysis by short-listing those which are most likely to produce the best results, viz. images which are relatively cloud-free, which have observable wave-fields (the greater the wave height, the better) and which have waves that travel at sufficient speed such that changes in phase can be easily detected (the longer, the better). The combination of these criteria makes the wave power ($\propto$ height^2×period) an obvious and effective proxy for selecting the best times for carrying out the analysis. As such, hindcast wave data from the European Centre for Medium-Range Weather Forecasts (ECMWF) ERA5 global dataset (Dee et al., 2011; Copernicus Climate Change Service (C3S), 2017) was used to determine the background wave conditions and cloud cover for each image of the 72 selected West Africa tiles between September 2015 and February 2020. The data was sorted to minimise cloud cover (top 50 per tile) and, subsequently, maximise the wave power (top 30 per tile). Wave power was chosen as an appropriate parameter to pre-select images based on the results of a multiple linear regression model, detailed in Appendix A.

For analysis in S2Shores, following Baba et al. (2021), each top-30 image is broken down into 36 18.3×18.3 km sub-images for parallel computation on a multi-core processor high-performance computing server (HAL, CNES). Depth estimates are produced on a 200×200 m output grid, with therefore just over 300,000 depth estimates per image (if completely covered by water). A global land mask at 150 m resolution, produced by the ESA Climate Change Initiative[3] (Lamarche et al., 2017), is used to identify land areas which are excluded from the computations. For a detailed explanation of the computational implementation of S2Shores, the reader is directed to Baba et al. (2021).

3.2. Depth estimation using the S2Shores algorithm

Depth estimates are produced according to the method outlined in Bergsma et al. (2019b, 2021), which uses a combined Radon and discrete fast-Fourier transform method (hereafter, RT and DFT), also known as Fourier-Slicing, to detect wave signals within a sub-window of the satellite image. Depth estimation is repeated for each sub-window around a point where one wants to know the depth (h). The sub-window should be large enough to contain 1–2 wavelengths (λ). Thus, a minimum window size of 300 m is used at the shoreline, and increases incrementally – following the formulation in Bergsma et al. (2019b) – up to a maximum of 900 m in areas farther from land (10 km), where depths are expected to be greater and wavelengths longer. The RT of the wave signal in the sub-window produces a sinogram of integrated pixel intensities per direction. The wave direction is determined as the angle corresponding to the maximum variance in the RT-sinogram. The DFT of the RT enables the spectral phase of the waveforms to be determined per direction, the difference of which ($\Delta\Phi$) can be found between several pairs of detector bands. Presuming that the wavenumber (k) is constant or near-constant over the sub-window, $\Delta\Phi$ can be seen as representative of $\omega(t)$, and given that the timing between the different detector bands (Δt) is constant, the wave celerity (c) can be determined as:

$$c = \frac{\Delta\Phi}{k\Delta t} = \frac{\Delta\Phi\lambda}{\Delta t} \tag{1}$$

For each wave-number or celerity pair, (2) can be solved for depth.

$$c^2 = \frac{g}{k}tanh(kh) \Leftrightarrow h = \frac{tanh^{-1}\left(\frac{c^2k}{g}\right)}{k} \tag{2}$$

Estimates of water depth, wave celerity, wavenumber (wavelength) and direction are output by the S2Shores algorithm at each point on an output grid with a resolution of 200 m. This output data is further treated as outlined in the section following.

3.3. Post-processing of bathymetry estimates

3.3.1. Vertical referencing

Water depth estimates from S2Shores are, firstly, vertically referenced to mean sea level. Tidal elevation relative to mean sea level is obtained using the FES 2014 model (Carrere et al. (2016)) for each Sentinel-2 tile. The expected tide elevation is extracted for each date and location, and subsequently uniformly subtracted from the S2Shores depth estimates.

3.3.2. Masking

Masks are applied to the S2Shores output to remove unreliable depth estimates, primarily associated with clouds. Cloud masks are created using a simple threshold on the NIR band, assuming the majority of NIR radiation is absorbed by water bodies and reflected by clouds. A threshold of 0.02 is used on the normalized NIR reflectance (c.f. Banks and Mélin (2015)) to identify cloudy pixels, and areas within 100 m of such pixels are also masked. This NIR cloud mask removes most dense/opaque clouds; however, light cirrus clouds are not easily detected. Therefore, pre-made cloud masks from the Sentinel-2 database (Copernicus Data Access Portal, 2020) are also used to augment the NIR cloud mask. An example of the application of the NIR and Sentinel-2 cloud masks is shown in Fig. 3.

Output data are also masked where unrealistic depth or celerity estimates occur. Given that the expected maximum (minimum) wave period is 25 (4) s, S2Shores should ideally detect wave celerity between 4 and 34 m/s (± 10%). Depth estimates should also range from a minimum of 1 m to a maximum corresponding to a third of the deepwater wavelength. Areas, where depth, celerity or wave period estimates are greater or less than these expected detection ranges, are removed from the analysis.

3.3.3. Composite and mosaic

In order to obtain a final bathymetry estimate for each of the 73 West Africa tiles, multiple images have to be used to create a composite in order to fill in potential data gaps caused by masking (similar to how a cloud-free image is created). Furthermore, a bathymetry composite created from an ensemble average of data at each point in the output grid is more robust than a single estimate, as it helps to minimise localized errors due to imperfections in the masks (for example, we can see that not all cloudy spots are completely removed in Fig. 3h–i). The best 10 of the 30 pre-selected images are used to create a depth composite for each tile. Three criteria are used to short-list the best 10 S2Shores results: 1) a *depth range score*, 2) usable data remaining after masking, and 3) correlation with GEBCO.

In the first step, we rank S2Shores depth estimates according to a *depth range score* and remove the lowest 7 images. The *depth range score* is calculated by comparing the depth ranges in the S2Shores results with the expected depth range from GEBCO in the target area of the image tile

[2] https://sentinel.esa.int/web/sentinel/missions/sentinel-2
[3] http://maps.elie.ucl.ac.be/CCI/viewer

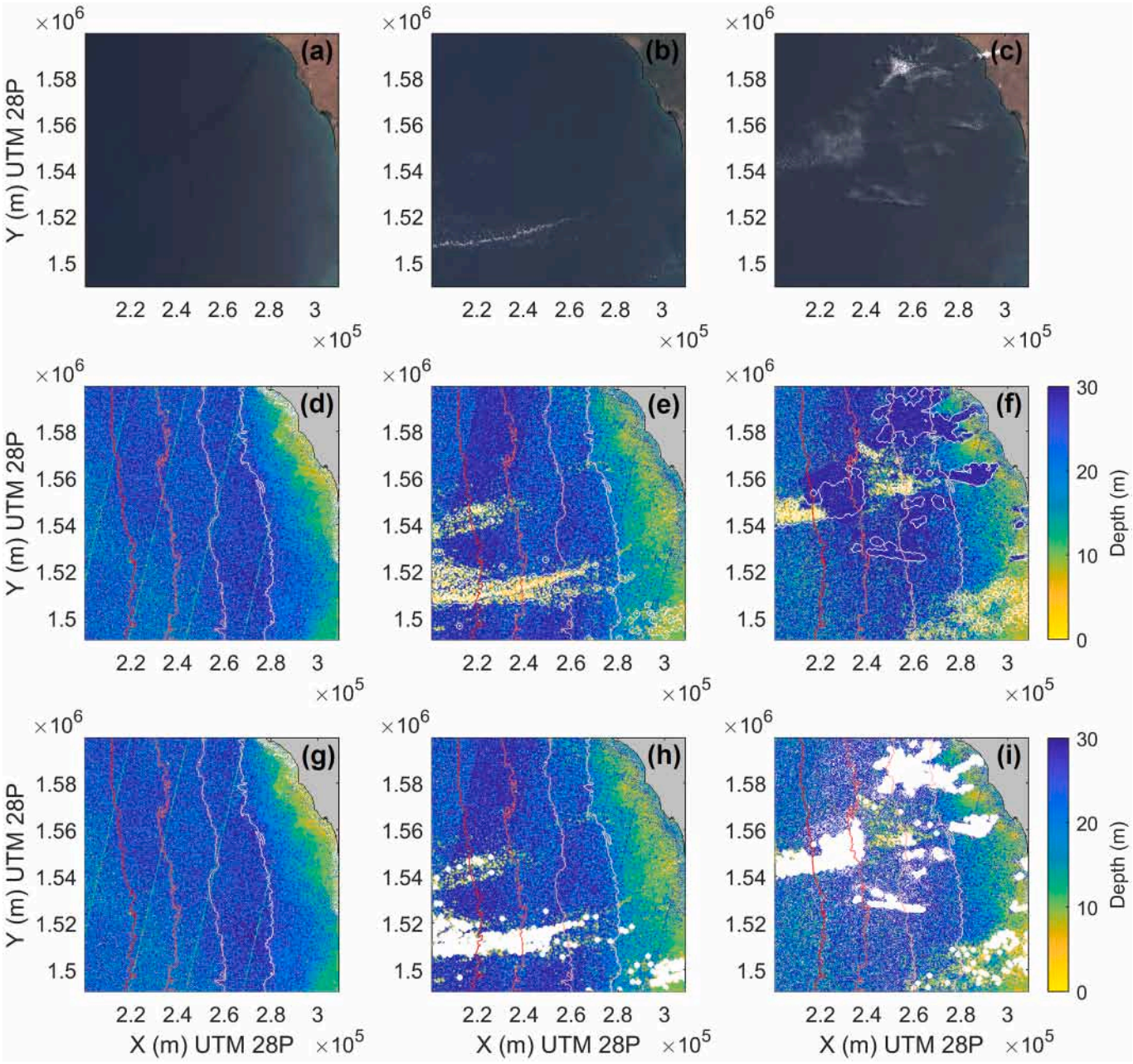

Fig. 3. An example of raw data output from the S2Shores algorithm. True colour images are shown for tile 28PBA (southern Senegal) taken on 13 April 2016 (a), 20 October 2017 (b) and 12 June 2018 (c). Image (a) is cloud-free, while (b–c) have mixed light and dense cloud cover. Raw output from S2Shores (panels d–f for each date, respectively) shows that depth estimates are degraded where there is cloud cover. Panels (g–i) show the result of applying cloud masks (also shown as while contour line in panels(d–f)). For reference, GEBCO depth contours (25, 50, 100 and 1000 m) are shown in (d–i) as shades from light pink (25 m) to red (1000 m). (For interpretation of the references to colour in this figure legend, the reader is referred to the web version of this article.)

where GEBCO depths range from 1 to 35 m. In doing so, therefore, GEBCO represents a first-order estimate of the expected depth range at a large scale (order of 100 km), given that it is mainly based on gravimetry. Small scale variations and features are not of interest at this stage.

The *depth range score* is based on the depth range corresponding to the difference between the 15^{th} and 85^{th} percentile depths for S2Shores and GEBCO in the target area. It is the ratio between the S2Shores and GEBCO depth ranges (the *depth range ratio*) that is scored on a scale between 0 and 1. *Depth range ratios* between 0.66 and 1.5 are scored at 1. The *depth range score* decreases linearly toward zero both as the *depth range ratio* tends downward to 0.1 from 0.66, and as the *depth range ratio* tends upward to 10 from 1.5. The *depth range score* is 0 elsewhere. This therefore favours S2Shores estimates that have fairly similar depth ranges as GEBCO at large scale, and eliminates those that significantly over- or under-estimate the expected depth range.

In the second step, we rank the S2Shores results according to most amount of data remaining after masking, and remove the lowest 7 images. In doing so, we favour S2Shores estimates that have the lowest cloud cover and thus the least amount of data gaps. In the third and final step, we rank according to the correlation with GEBCO and remove the lowest 6 images, ensuring the best images are used to create the composite. The correlation is determined in the target depth area between 1 and 35 m over the image tile.

Once the best 10 S2Shores depth estimates have been short-listed, the weighted average of the depth at each point in the output grid is found. The weighted average is normalized by the correlation with

GEBCO, with more highly correlated depth estimates contributing more to the average. It should be noted that the weighted average is only computed once there are more than 3 valid data points after masking (if less, the depth is left blank). The final step in creating the composite is to smooth the (temporally) weighted depth at each output point with neighboring points in space (within 2 grid cells, or a 400 m radius) using a median filter in order to reduce the appearance of artifacts. The final 73 depth composites are then tiled together to create a depth mosaic for the entire study area.

3.4. Comparative bathymetry datasets

S2Shores depth estimates have to be compared to measured data to determine its quality. Besides GEBCO, publicly available coastal bathymetry datasets are difficult to source for the study area and tend to be quite dated. Privately held data at the French Naval Hydrographic and Oceanographic Service (SHOM) was obtained for the Senegalese coast (hereafter referred to as the 'available data'), but not for the remaining portions of the West African coast. Therefore, comparisons made with the available data at the Senegal hot-spot will help to show the accuracy of the S2Shores results, while more general comparisons with GEBCO are made elsewhere. The spatial resolution of GEBCO data is 0.0042° (approximately 460 m at the equator). This means that for comparison to S2shores output, GEBCO data is down-scaled to the S2Shores 200 m output grid by interpolation.

4. Results

4.1. Regional West African bathymetry

S2Shores estimates of the regional West African bathymetry are shown as a mosaic for all 73 selected Sentinel-2 coastal tiles (Fig. 4). Depths are shown up to a distance of 15 km offshore, or to the extent of the 50 m contour line in GEBCO (whichever is greater). At this scale, it is possible to observe the extent of the upper, shallow portion of the shelf. It is widest between Guinea-Bissau and Sierra Leone, and at the Niger Delta, and most narrow between Liberia, Ivory Coast and Ghana. Deep features (> 30 m depth, such as submarine trenches) are not easily distinguished from the general background. However, more shallow features, such as ebb delta channels around the Bissagos Islands (Guinea-Bissau) and the St. Ann's Shoal in Sierra Leone are captured very well.

4.2. Illustrative zoom at hot-spots

Six 'hot-spots' are identified within the AoI, covering a varied range of coastal types. They are, namely, Senegal, Guinea, Sierra Leone, Volta Delta, Niger Delta, and Cameroon. The hot-spots are excellent test sites for the S2Shores algorithm because of the diverse range of coastal features, wave exposure and cloud cover at each location.

Fig. 5 shows close-ups of the S2Shores depth composites at the six hot-spots compared to GEBCO, highlighting the ability of the model to discern depth patterns at a sub-regional scale. Here, the data is shown at 200 m resolution and (at least) out to the 50 m GEBCO depth contour. To highlight even more detail of the resulting S2Shores bathymetry estimates, Fig. 6 zooms in further to the scale of a single tile at each hot-spot, and then further to a local 15×15 km area to highlight significant

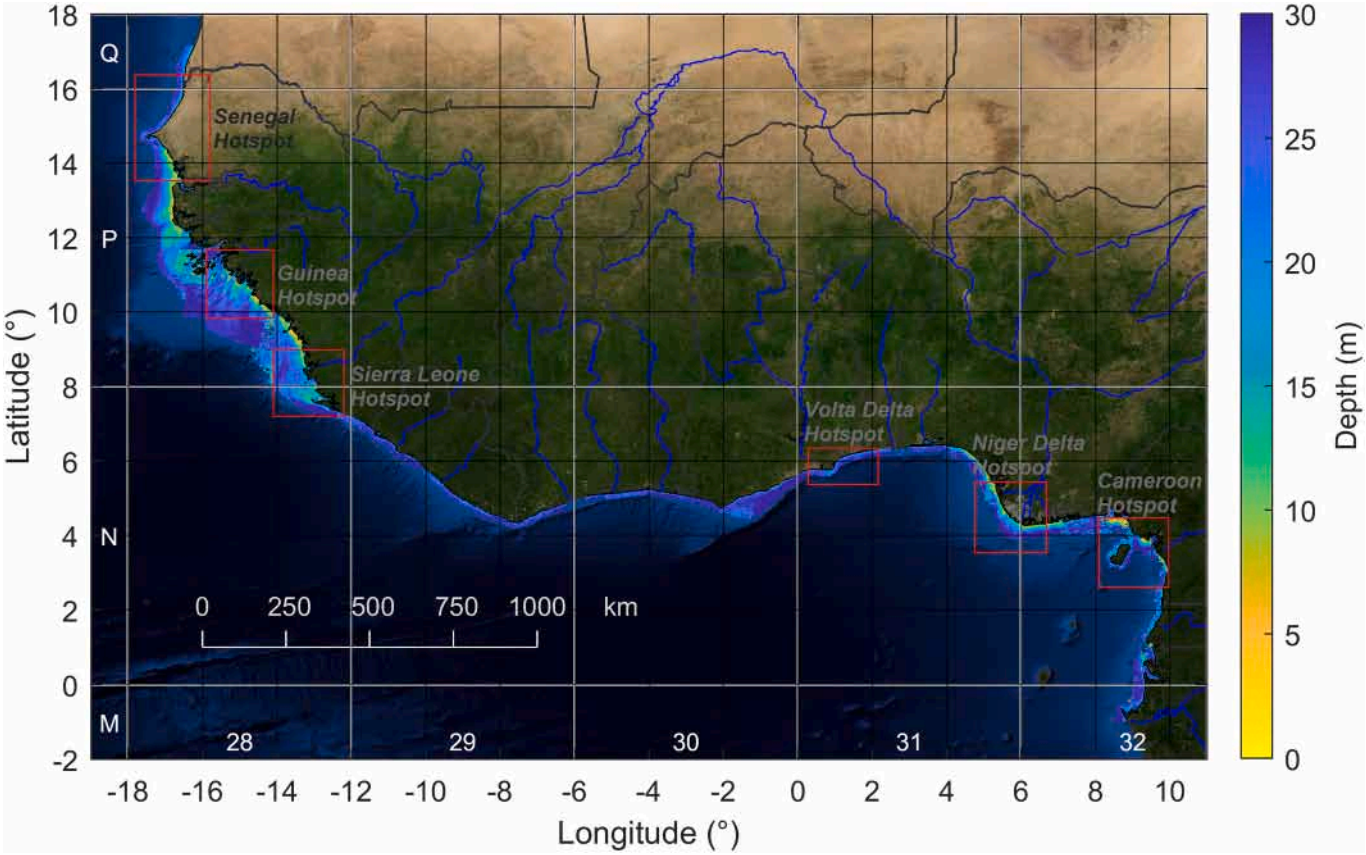

Fig. 4. Mosaic of S2Shores bathymetry composites for the West Africa Region. Colour scale shows depths between 0 and 30 m, the black line shows the shoreline, and UTM zone boundaries shown in white. Red boxes outline the area of the six hot-spots. *Background image: MODIS Blue Marble, NASA Earth Observatory.* (For interpretation of the references to colour in this figure legend, the reader is referred to the web version of this article.)

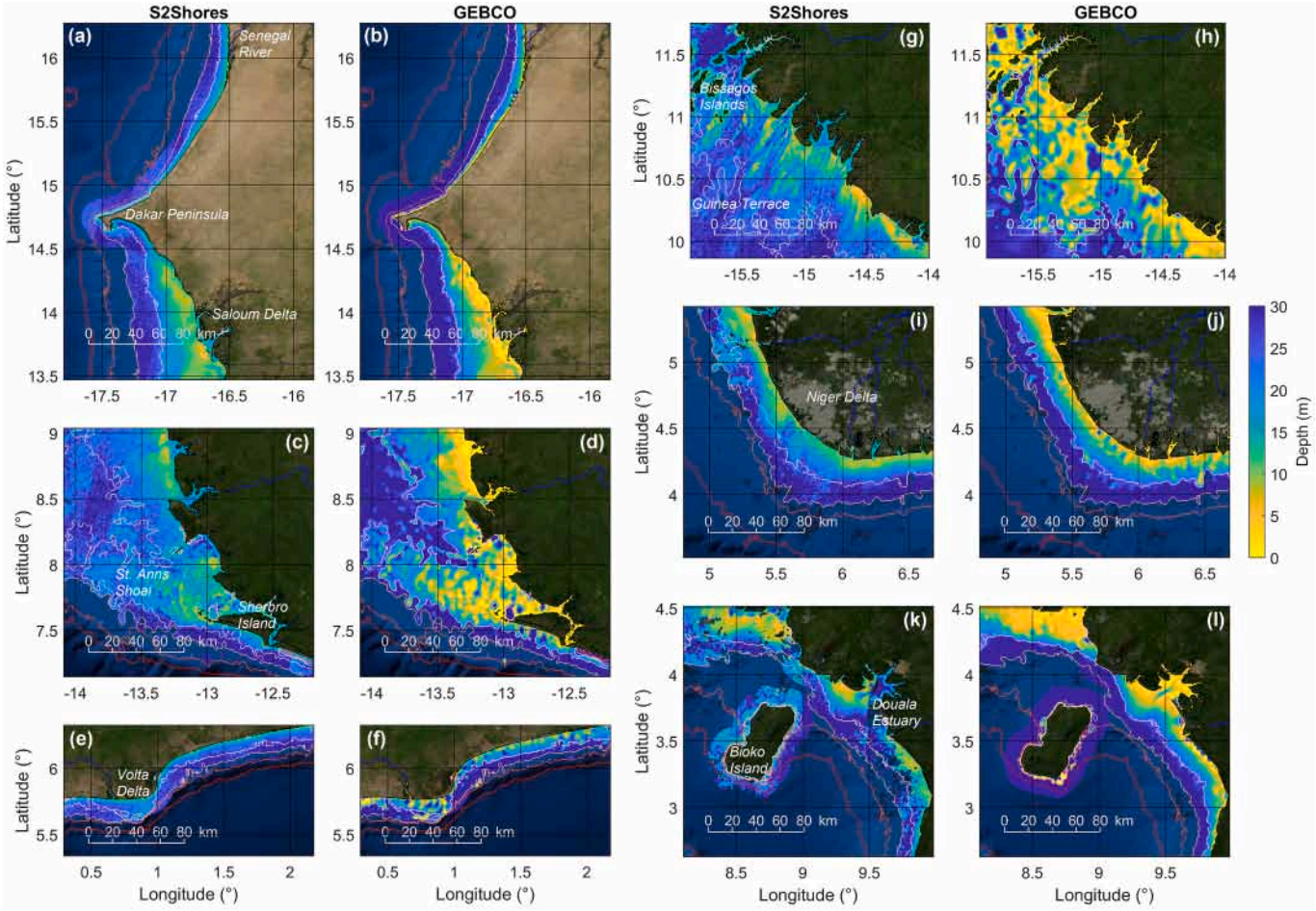

Fig. 5. Comparison between S2Shores bathymetry composite and GEBCO for the six hot-spots. (a-b) Senegal (tiles 28PCC, 28PBB, 28PBA, 28PBC and 28PCA). (c-d) Sierra Leone (tiles 28PFQ, 28PGQ, 28NFP and 28NGP). (e-f) Volta Delta (tiles 30NBG and 30NCG). (g-h) Guinea (tiles 28PDS, 28PTS, 28PET and 28PDT). (i-j) Niger Delta (tiles 31NHE, 31NGE and 31NGF). (k-l) Cameroon (tiles 32NNK, 32NNJ, 32NMK and 32NMJ). Colour scale shows depths between 0 and 30 m, and the shoreline is traced in black. For reference, GEBCO depth contours (25, 50, 100 and 1000 m) are shown as shades from light pink (25 m) to red (1000 m). *Background image: MODIS Blue Marble, NASA Earth Observatory.* (For interpretation of the references to colour in this figure legend, the reader is referred to the web version of this article.)

shallow water features. Some of these shallow water features between 1 and 15 m are well detected by S2Shores, such as flow channels in Guinea, the St. Ann's Shoal in Sierra Leone, and ebb delta lobes at several outlets along the Niger River Delta.

The best comparison between GEBCO and S2Shores is at Senegal (Fig. 5 a–b). As mentioned in Section 3, this section of the West African coast is exposed to long-period Atlantic swell. This, coupled with low cloud cover on average, allows S2Shores to predict smooth transitions from deep to shallow water. The area immediately south of the Dakar peninsula is well-predicted, despite it causing some degree of wave shadowing for incident wave fields from the north. The shallow area of the remaining portion of the coast in the south broadens as expected, heading toward the deltaic region of Guinea-Bissau. Maximum depth estimates at this location are approximately 30 m.

At the Sierra Leone and Guinea hot-spots (Fig. 5 c–d and g–h), shallow features present on the wide continental shelf are detected by S2Shores. Channel features at the Guinea hot-spot are more clearly resolved by S2Shores than GEBCO, although they appear deeper. GEBCO depths for the same area are spotty and irregular, with little semblance of natural flow channels. The defining shallow water feature at the Sierra Leone hot-spot is the St. Ann's shoal, located north-west of the Turtle and Sherbro Islands. Here, rhythmic underwater dune features are discernible in the S2Shores results, with heights between 8 and 12 m and wavelengths of 6–7 km. Predicted S2Shores depths on the wide continental shelf around the Guinea and Sierra-Leone hot-spots are limited by its inherent shallowness, with depth saturation around 26 m. However, the southern edge of the shelf in Sierra Leone is clearly shown down to depths of 33 m.

Maximum depth estimates at the Cameroon hot-spot (Fig. 5 k–l), located in the Bight of Bonny, are around 30 m. This area generally has lower wave periods and a considerable reduction in usable data after cloud masking compared to other hot spots. However, despite the year-round high cloud cover, quite good estimates of shallow nearshore banks at the entrance to the Wouri estuary are obtained, as can also be seen in GEBCO (Fig. 6k). On the other hand, high cloud cover does affect depth estimates in other areas, enough to leave data gaps in certain spots after masking (e.g. Fig. 6k). Depths along the narrow shelf around Bioko Island (Equatorial Guinea) show a transition from deep to shallow on the eastern side of the island, but not on the western side where, in fact, they deep areas are predicted to be shallow.

At the Volta Delta, S2Shores shows similar depth patterns as GEBCO around the offshore apex of the delta. The shelf is wider in the west, extending up to 20 km offshore, and is about 10 km in the east. S2Shores is able to sense depths down to around 30 m, and detects where there is a sharp change in depth at the shelf edge, which starts to drop steeply after 25 m depth (Fig. 6g–h). The Niger Delta area is also nicely estimated by S2Shores, with deep channels seen at the mouth of the Niger river at Forcados, and crescent-shaped outer delta lobes at several other mouths

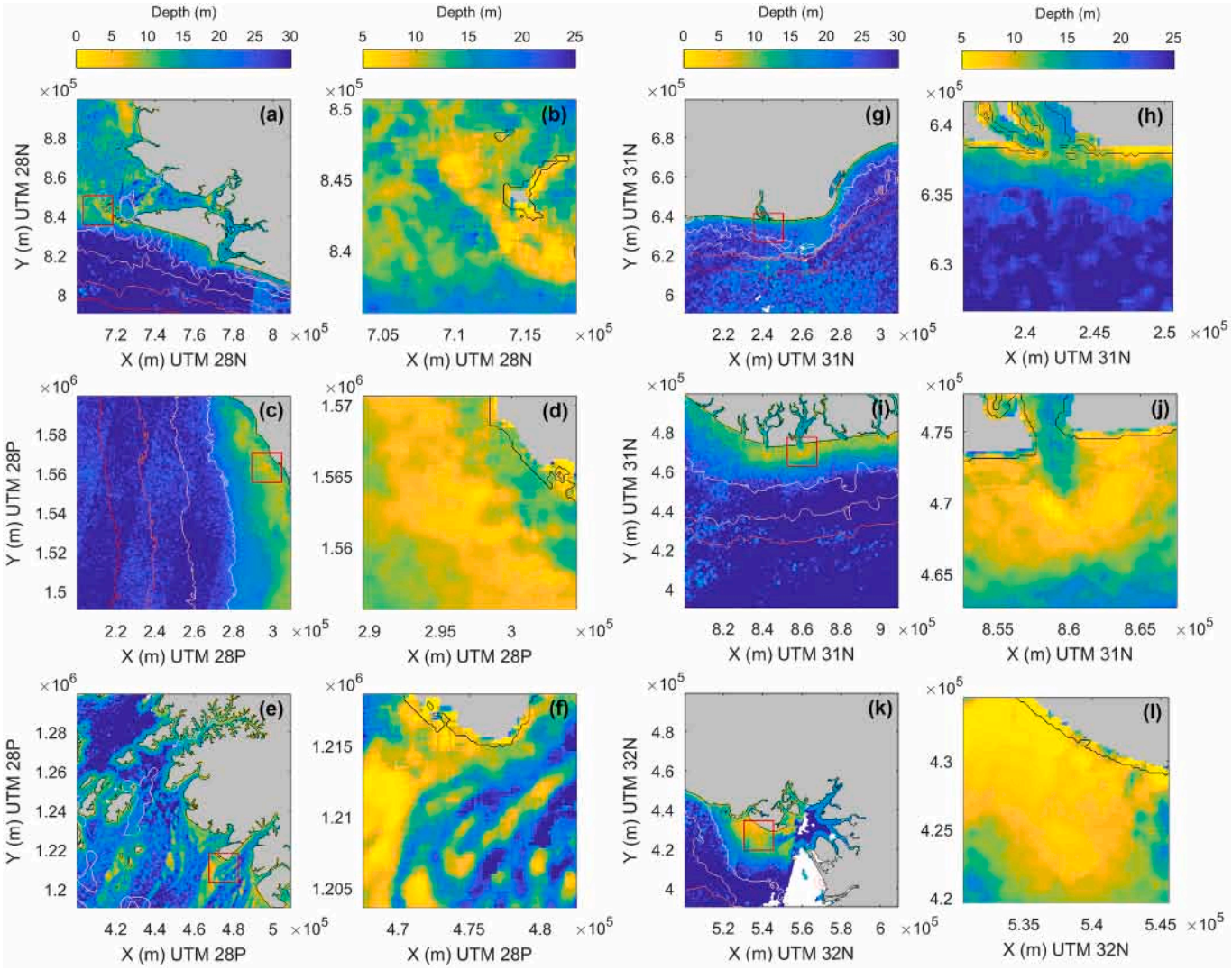

Fig. 6. Illustrative S2Shores bathymetry highlighting local features at each of the 6 hot-spots. Columns one and three (a, c, e, g, i and k) show composite depths results at tiles 28NGP, 28PBA, 28PDT, 31NBG, 31NHE and 32NNK, located at the Sierra Leone, Senegal, Guinea-Bissau, Volta Delta, Niger Delta and Cameroon hot-spots, respectively. The red squares indicate an area of 15×15 km, shown in further detail in columns two and four (b, d, f, h, j and l) for each hot-spot, respectively. For reference, GEBCO depth contours (25, 50, 100 and 1000 m) are shown in columns one and three as shades from light pink (25 m) to red (1000 m). The colour scale shows depths between 0 and 30 m for each image tile (columns one and three) and between 5 and 25 m at the local zoom (columns 2 and 4). The black line shows the shoreline and grey shaded areas are land. White areas indicate locations where there was insufficient data to generate a composite depth after masking. (For interpretation of the references to colour in this figure legend, the reader is referred to the web version of this article.)

such as at Digatoro, Sangan, Nun and Brass (Fig. 6i–j). Shallow areas (down to 20 m) tend to be slightly over-predicted compared to GEBCO, and depths begin to saturate at around 33 m.

4.3. Quantitative comparison with bathymetric data at Senegal

The quality of the S2Shores results is assessed by comparing output at the Senegal hot-spot to the available independent bathymetric data. High correlation coefficients (r^2) are obtained for depths between 1 and 35 m, with a value of 0.76 when compared to the available data. For the same depth range, RMSE is 4.9 m and the linear best-fit has a gradient of 0.62 and an intercept of 8.1 m. A scatter plot of the results in Fig. 7 show that S2Shores tends to overestimate very shallow depths < 10 m. Offshore depths in S2Shores also become saturated at around 30 m, beyond which it will largely underestimate the true depth. This response is expected, however, as ever longer waves are required to sense small changes in celerity in deeper water. Despite this, depths between 10 and 30 m are fairly well predicted, where majority of the depth estimates lie close to the target depth. There, the absolute error is approximately 18% of the target value on average, with the RMSE and bias being 4.0 and 1.3 m, respectively.

4.4. Qualitative comparison with chart data

Qualitative assessment of S2Shores results can be made by comparing it to the position of 10, 20 and 30 m depth contour lines from chart data.[4] Available chart data only covers a very small portion of the area of interest, in parts of Gabon, Guinea, Nigeria, and Togo (Fig. 8). Given the limited coverage of the chart data, it does not give an overall view of the performance of S2Shores, but is still useful to note areas where it may or not perform well.

For locations along the coast of Gabon, S2Shores depth estimates around 10 m (interface between green and yellow patches) correspond quite well with the 10 m chart data contour (Fig. 8a, b), where

[4] The authors have only obtained permission to reproduce small segments of the original charts.

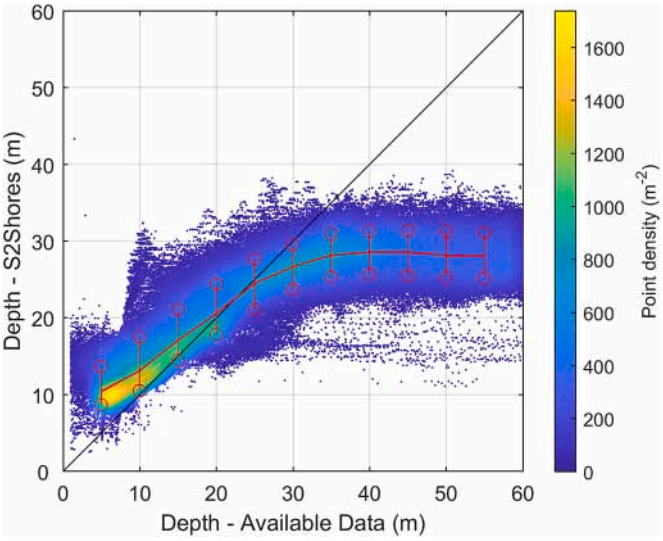

Fig. 7. Scatter plot of S2Shores depth estimates against available data at Senegal. Black line indicates the target depth (1:1 comparison), the red line shows the mean trend of the S2Shores estimates in 5 m-wide bins, and the red circles show the standard deviation about the mean of each bin. Over the 1-35 m range, $r^2 = 0.76$ and RMSE = 4.9 m. Colour scale indicates the density of points within a 1 m^2 area of the plot. (For interpretation of the references to colour in this figure legend, the reader is referred to the web version of this article.)

horizontal offsets generally range between 0 and 5 km. Along 30 km of the coast at Lomé, Togo, the 10 m chart data contour line lies approximately 5 km onshore of S2Shores predictions. S2Shores performs poorly in some sheltered areas, such as Iles de Los, Guinea (Fig. 8c). There, S2Shores largely overestimates shallow depths (<5 m) due to wave shadowing from the island archipelago. Along 110 km of the coast of the Niger Delta, Nigeria (Brass to Bonny River), the 10 m chart data contour lies within 2 km of S2Shores estimates (Fig. 8f), but in other areas (Pennington to Nun River), it is up to 10 km offshore (Fig. 8e). While these results therefore indicate mixed performance of S2Shores, it also highlights the need for greater availability of measured bathymetric data to further validate the performance of the S2Shores algorithm.

5. Discussion

5.1. Depth application range

Our results show that S2Shores is able to detect depths down to 35 m (where we observe a deep water plateau), as is the case for Senegal which generally experiences long swell and generally low cloud cover for most of the year. Furthermore, the estimation of depth over such a large area for the West African coastal zone, O(100,000 km^2), is quite unique for SDB methods, which are normally carried out in very localized areas O(1,000 km^2). For the hot-spots, depths between 10 and 30 m are well estimated and many shallow underwater features are apparent. This limit goes beyond Lidar observed penetration over regional scale which extends up to 26 m Thomas et al. (2021) and with colour-based methods around 15 m for non-clear waters (Stumpf et al., 2003; Lyzenga et al., 2006; Lee et al., 2010; Hodúl et al., 2018).

The deepwater limit of 35 m found here is less than the theoretical limit of approximately 55 m for West Africa, under ideal wave conditions (Bergsma and Almar (2020)). This reduction in the offshore limit is partly due to the small number of images used in creating the depth composite (only 10), but also the effect of masking out clouds, as shown in Bergsma and Almar (2020). If a larger number of observations were used in making the composite, the probability of retrieving better deepwater estimates under ideal wave conditions would be increased. This is an issue of limited computational resources rather than the method itself.

In addition, the underestimation in deep water is also due to the fixed size of the average computational window, which automatically prevents capturing the longest waves. In addition, shorter waves have a stronger signature than longer, relatively flat waves, resulting in a higher weight in the wave spectrum, which may influence the peak frequency taken by our spectral method to invert the depth and thus the underestimation. All of these factors combined result in a plateau around 35 m in our data. In addition, any inaccuracy in the wave parameters leads to large discrepancies in the estimate of deep water bathymetry. The overestimation of the shallowest areas is due to the

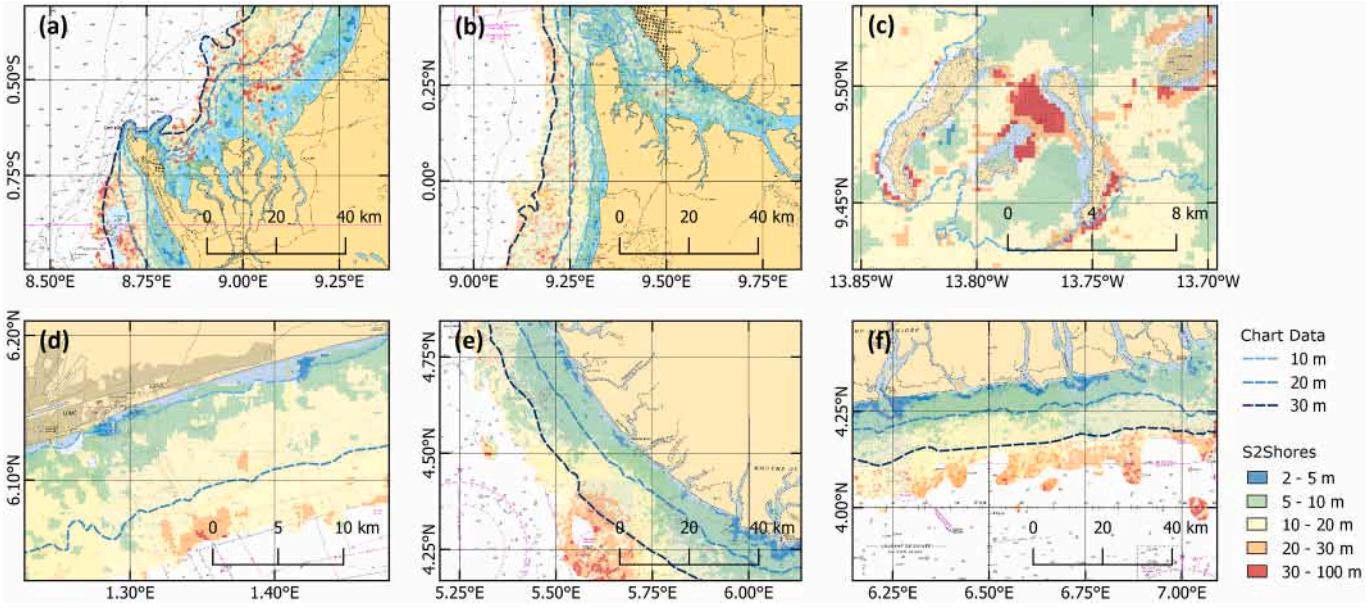

Fig. 8. Comparisons between S2Shores results and available chart data for: (a) Port Gentil, Gabon; (b) Libreville, Gabon; (c) Iles de Los, Guinea; (d) Lomé, Togo; (e) Pennington to Nun River, Nigeria; and (f), Brass to Bonny River, Nigeria. S2Shores data is classified in colour bands (blue to red), while contour lines (10, 20 and 30 m) shown from chart data for reference. (For interpretation of the references to colour in this figure legend, the reader is referred to the web version of this article.)

optical artifact of the land and wave breaking which is similar to the actual incident waves but with a longer signal.

As seen in the results, S2Shores tends to overestimate depth in very shallow water. This is caused by a number of factors, most importantly 1) perturbations from the shoreline found within the computational sub-window (~1 km^2), 2) varied pixel intensity maxima around areas of wave breaking, 3) limitations of the 10 m Sentinel-2 pixel footprint in determining changes in wave phase, especially in areas where waves travel at sub-pixel speeds. These factors tend to lead to false estimates of deep-water in areas that are shallow, and can affect neighboring points when spatial smoothing is done over a large area. This effect is seen in Fig. 6c–d at tile 28PBA, where depths get shallower moving onshore, then deeper again just around the shoreline. Additional techniques to account for these issues can be implemented, as are currently being studied by Bergsma et al. (2021).

5.2. Comparison with colour-based methods

Colour-based SDB methods are able to detect depths in shallow areas up to 15 m deep, and with exceptionally fine resolutions around 5 m. Absolute errors are generally 18% of the target value, with an average RMSE of 1.5 m (Pacheco et al., 2015; Ch´enier et al., 2018; Traganos et al., 2018). On the other hand, the detectable depth range for S2Shores is 2.5 times greater than the typical range of colour-based SDB methods (Caballero and Stumpf, 2019); however, S2Shores currently largely overestimates depths in shallow water <10 m. These estimates largely improve in intermediate water (10–30 m), where absolute errors are within 18% of the target depth and RMSE is 4 m. S2Shores depth estimates can be output at resolutions down to 50 m, but would require significant computational effort when applied over a very large area.

The real difference between the wave-based and colour-based SDB methods perhaps does not come from their error values, but rather on their application. The S2Shores algorithm works well in conditions where colour-based methods would fail, namely in turbid or optically deep water (which is most of the West Africa coastline). But at the same time S2Shores would fail in environments where colour-based methods work well; namely in archipelagos, behind reef crests, in narrow bays, fjords, and other closed environments sheltered from waves. The finer resolution of colour-based SDB data would allow sharp changes in depth to be better resolved, especially since wave-based methods are inherently physically limited by the wavelength and the time for waves to respond to a varying bottom.

Given that both methods are fairly similar in terms of accuracy, they can be used in combination to detect bathymetry from very local to regional scales, since where one method may fail the other would work well. This would permit exceptional coverage of diverse coastal conditions from shallow to relatively deep waters.

5.3. Dependency of quality on meteorological conditions

The S2Shores algorithm produces useful estimates once a distinct wave-field can be observed. The mean period of swell waves, the wave power, directional spreading, and cloud cover are among the most influential parameters affecting the quality of the S2Shores estimates (see detailed analysis in Appendix A). Powerful swell waves (with large heights and long wavelengths/periods) travel faster than the background wind waves and are more easily detected in the algorithm (Bergsma et al., 2019a). These waves also allow for deeper estimates of depth. Narrow banded swell reduces potential cross-sea patterns, which may create multiple peaks in the directional space of the pixel intensity. Furthermore, short steep waves (even if they are less energetic) may have a larger optical signature than longer, flatter waves, which can result in an under-estimation of the depth (Almar et al., 2021a). While opaque clouds block the view of the sea surface, light cirrus clouds, fog or atmospheric dust also obscure the field of view and lead to unreliable depth estimates.

5.4. Perspectives

The ability to frequently and accurately monitor bathymetric changes over large scales will significantly help to broaden our understanding of dynamic coastal processes and their coupling to large-scale forcing conditions (Bergsma et al. (2022)). While we have currently used images taken within a 5-year period, S2Shores composites computed over shorter time periods will offer the possibility to create unique time series of bathymetry and thus observe dynamic changes of shallow water features, such as delta formations or underwater dune migration. As such, annual, seasonal or even monthly depth composites can be generated.

Decreasing the period over which images are used to construct a composite would tend to reduce the signal to noise ratio, as the probability of occurrence of successive high energy wave conditions (and jointly, low cloud cover) over a shorter space of time is reduced. The ability to detect bathymetric changes also depends on the local depth of closure (Bergsma and Almar (2020)), as such changes tend to be more rapid in shallow rather than deep water. Nonetheless, depth changes may still be detected over the entire water column at various timescales with adaptive windowing.

Finally, the 73 Sentinel-2 tiles selected for the West Africa atlas represents 1% of the global list of Sentinel-2 coastal tiles with depths up to 100 m. With such promising results as shown, there is definite potential for the method to be further applied on a global scale Almar et al. (2021b). The spatial resolution of the estimates may also be decreased from the 200 m used for this study. For instance, initial tests were carried out on a 100 m grid. A lower limit of 50 m is possible, and would potentially permit the visualisation of bottom features such as sandbars. However, it would come at a much higher computational cost, and would therefore be more suited for generating datasets at a local level.

6. Conclusion

Most coastal areas in the world suffer from a lack of bathymetry data, with no or decades-old observations. Satellite Earth observation opens the new era of measuring coastal bathymetry from space. Commonly used colour-based depth inversion methods are often limited in turbid coastal areas. However, the recently developed S2Shores algorithm, based on extracting wave kinematics from within Sentinel-2 multi-spectral image bands, has been used to produce unprecedented fine resolution O(100 m) regional-scale coastal bathymetry from satellite along 4000 km of the West African coastline and almost 70% of the coastal zone of the continental shelf. The method is able to detect depths down to 35 m, and while shallow depths below 10 m tend to be over-estimated at present, intermediate waters between 10 and 30 m are fairly well estimated. Future work will investigate the potential of the method to monitor the dynamics of coastal features, such as deltas, shoals and underwater dunes. This new Coastal Atlas of West Africa opens the door to increased research and planning capabilities for the region, and sets an example that can be applied to the rest of the world, on a regular basis.

Author contributions

Conceptualization: RA and EB. Methodology and Data Processing: EB, WB, GT and CD. Data Analysis and Interpretation: CD. Writing – Original Draft: CD. Writing – Review and Editing: All authors. Project Administration and Funding: RA and TG.

Declaration of Competing Interest

The authors declare that they have no known competing financial interests or personal relationships that could have appeared to influence the work reported in this paper.

Acknowledgements

This study was carried out as part of the project MEPELS, performed under the auspices of the DGA, and led by SHOM. E.B. was funded through a post-doctoral fellowship of the French National Centre for Space Studies (CNES). The authors would like to thank members of the PEPS and HAL teams at the CNES Calculation Center, especially Christophe Taillan, Erwann Poupart, Guillaume Eynard-Bontemps, Florent Ventimiglia, and Sylvain Rigole, for providing technical support in accessing the Sentinel data products and developing parallel computing scripts for the CNES High Performance Cluster. The authors would also like to thank the three anonymous reviewers for their valuable comments and feedback which greatly helped to improve the quality of the manuscript.

Appendix A

As mentioned in §3.1, images are pre-selected from the Sentinel 2 image database based on minimizing cloud cover and maximising wave power. However, there are certain aspects of the (oceanic) wave field and (atmospheric) weather patterns that may (or not) contribute to providing good conditions for which bathymetry may be extracted. Here, we further assess which wave and weather (i.e. meteorological) parameters have discernible impacts on the quality of S2Shores results, and what are the best methods to describe the related depth errors.

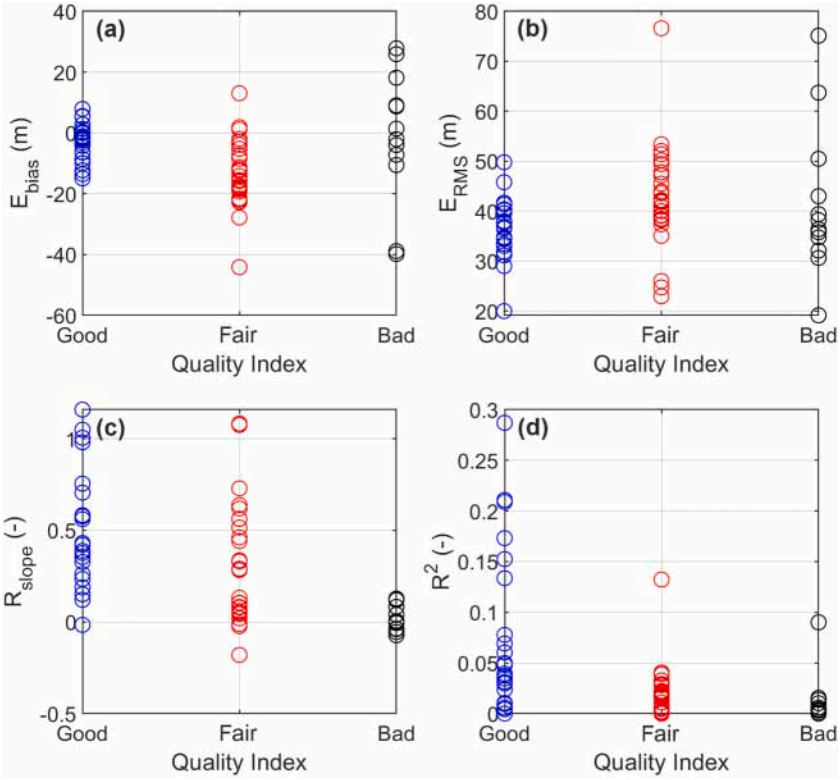

Fig. A.9. Comparison of qualitative and quantitative error descriptors for 1 year's worth of S2Shores depth estimates at the Senegal hot-spot. Panels a-d show bias (E_{bias}), root-mean-square error (E_{rms}), linear regression slope (β), and correlation (r^2) values, respectively, classified as 'good', 'fair' and 'bad'.

Firstly, one years' worth of Sentinel-2 observations (January 2018 to January 2019) at the Senegal hot-spot were analysed (72 images tiles at 28PCC). Quantitative errors for S2Shores depth estimates relative to available data were calculated using several descriptors, namely the bias (E_{bias}), root-mean-square error (E_{rms}), coefficient of determination (r^2), and slope of the linear regression (β). Cloud masks were applied to the input data and errors were computed in locations where S2Shores estimates were <100 m (i.e. the theoretical depth limit of the S2Shores method). A qualitative description of the error was also attached to each depth estimate to signify whether the S2Shores result was 'good', 'fair' or 'bad'. 'Good' estimates had clear transitions of depth from shallow to deep, 'fair' results tended to be monotonous, and 'bad' results had significant depth artifacts (mainly as a result of high cloud cover coupled with imperfect cloud masks). Fig.A.9 shows that 'good' estimates tend to have lower E_{bias} and E_{rms} values and higher β and r^2 values compared to 'fair' or 'bad' estimates.

Further, several meteorological parameters were defined from wave and weather data available from the ERA5 database (Dee et al., 2011; Copernicus Climate Change Service, 2017). Base parameters include the total significant wave height (H_s), peak wave period (T_p), mean wave period (T_m), zero-crossing wave period (T_z), wave energy (E), wave power (P), wave direction (D), directional spreading (D_{spr}), wave steepness (S), wind speed (W_{10}), and wind direction ($W_{10,\ dir}$). Base parameters related to waves were further separated into wind sea and swell components (denoted by subscripts w and s). Additional parameters were computed, namely the differences between wind and wave directions, and the ratios of E, P and H_s between wind sea and swell conditions.

A total of 30 defined meteorological parameters were input in a multiple linear regression (MLR) model to determine the strength of their relationship with each of the four defined quantitative S2Shores error parameters, and thus, to determine which are most influential. Results from the MLR analysis rank each of the defined meteorological parameters using correlation coefficients. r^2 values above 0.25 indicate that a significant portion of the variance in the error parameter can be explained by a certain meteorological parameter. From this analysis, the only error descriptors which have associated meteorological parameters with $r^2 > 0.25$ in the MLR model are E_{bias} and r^2. The parameters recognised as contributing most to the S2Shores E_{bias} and r^2 error estimates are $H_{s,\ s}$, T_z, $T_{m,\ s}$, E, E_s, P, P_s, and D_{spr} (Fig.A.10).

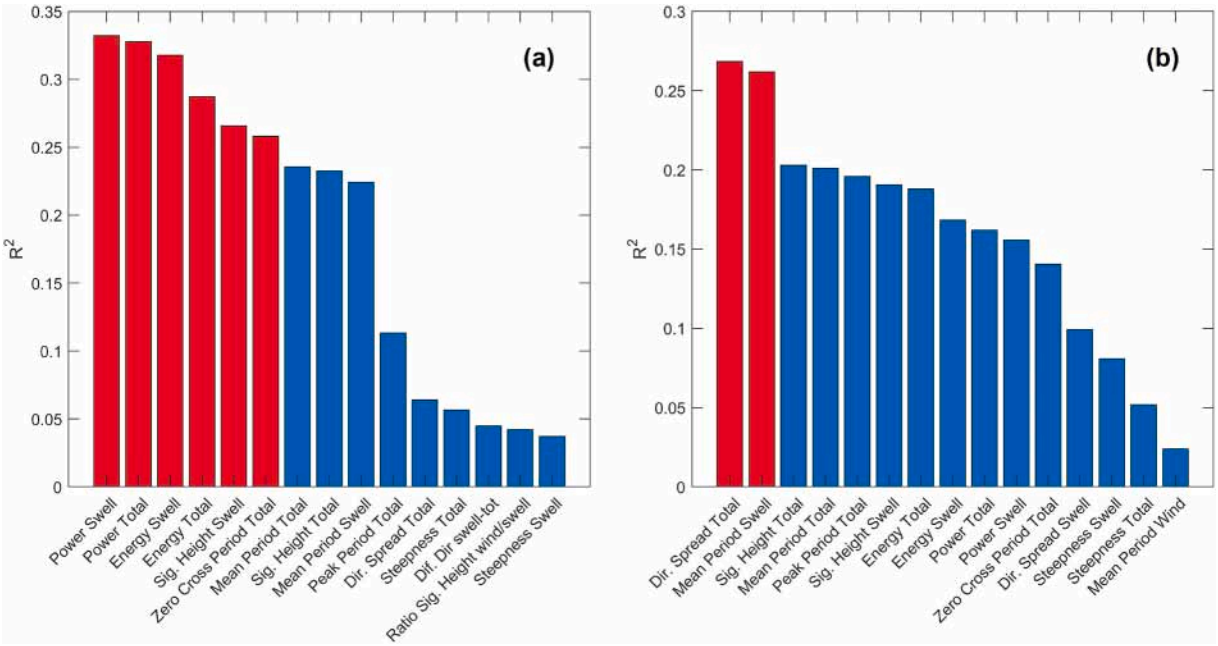

Fig. A.10. Result of the MLR model between defined meteorological parameters and S2Shores error parameters r^2 (panel a) and E_{bias} (panel b) at the Senegal hotspot. Red bars indicate meteorological parameters which significantly contribute to the variance of the defined S2Shores error parameters. Only the top 15 meteorological parameters are shown in each case. (For interpretation of the references to colour in this figure legend, the reader is referred to the web version of this article.)

The MLR therefore indicates that the presence of energetic, swell type conditions with low directional spreading produce the best results in S2Shores. Furthermore, clear differences between the average values of estimates quantitatively classified as 'good' and 'fair' can be seen when the 8 significant meteorological parameters are plot over time (Fig.A.11 a-h). Certain other parameters, such as W_{10}, do not produce clear distinctions between the quality of the result (Fig.A.11 i). In conclusion, wave power was selected as the parameter to define appropriate wave conditions to be run in S2Shores (in addition to low cloud cover) for locations in our area of interest in West Africa, especially as it is strongly related to other important parameters such as wave energy, height and period. While the analysis is specific to the Senegalese coast, we assume that the findings also generally apply to the entire area of interest.

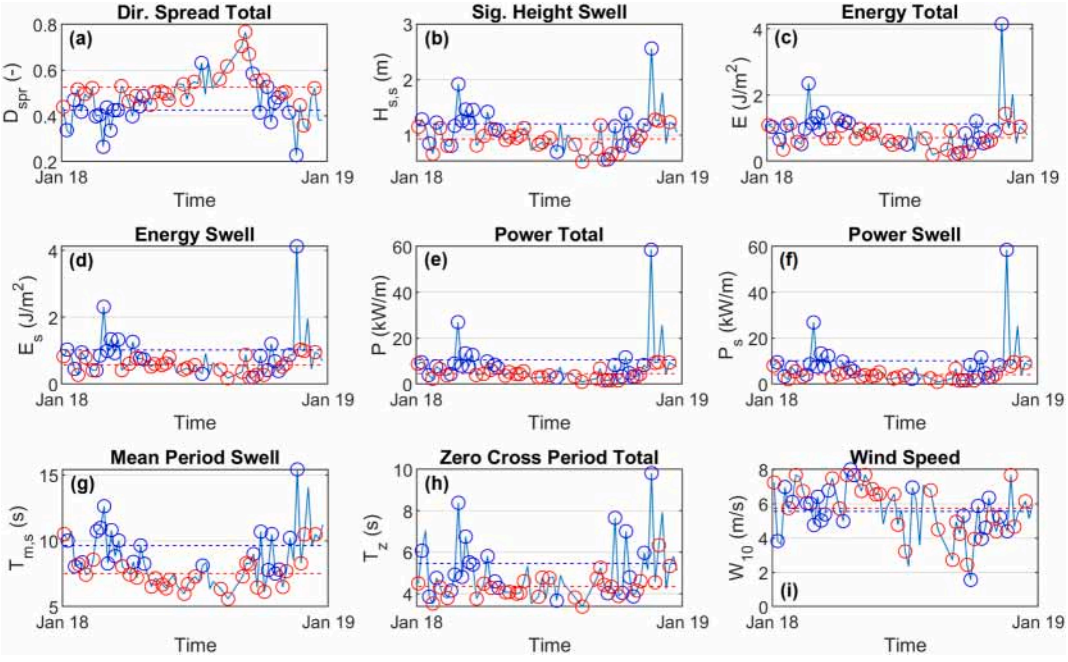

Fig. A.11. The top 8 meteorological conditions identified from the MLR model plot as a function of time (panels a-h, D_{spr}, $H_{s,s}$, E, E_s, P, P_s, T_z, and $T_{m,s}$, respectively). Panel i shows W_{10}. Blue and red circles represent times where the depth estimates were classified as 'good' and 'fair', respectively. The blue and red dashed lined indicate the mean value of the 'good' and 'fair' depth estimates, respectively. (For interpretation of the references to colour in this figure legend, the reader is referred to the web version of this article.)

References

Abdallah, H., Bailly, J.S., Baghdadi, N.N., Saint-Geours, N.N., Fabre, F., 2013. Potential of space-borne LiDAR sensors for global bathymetry in coastal and inland waters. IEEE J. Sel. Top. Appl. Earth Obs. Remote Sens. 6, 202–216. URL. https://hal.archives-ouvertes.fr/hal-01521998. https://doi.org/10.1109/JSTARS.2012.2209864.

Almar, R., Kestenare, E., Reyns, J., Jouanno, J., Anthony, E., Laibi, R., Hemer, M., DuPenhoat, Y., Ranasinghe, R., 2015. Response of the bight of Benin (gulf of guinea, west africa) coastline to anthropogenic and natural forcing, part1: wave climate variability and impacts on the longshore sediment transport. Cont. Shelf Res. 110, 48–59.

Almar, R., Bergsma, E.W.J., Maisongrande, P., Almeida, L.P.M., 2019a. Wave-derived coastal bathymetry from satellite video imagery: a showcase with pleiades persistent mode. Remote Sens. Environ. 231, 8 pp.

Almar, R., Kestenare, E., Boucharel, J., 2019b. On the key influence of remote climate variability from tropical cyclones, north and south atlantic mid-latitude storms on the senegalese coast (west africa). Environ. Res. Commun. 1 https://doi.org/10.1088/2515-7620/ab2ec6, 11 pp.

Almar, R., Bergsma, E.W.J., Catalan, P.A., Cienfuegos, R., Suarez, L., Lucero, F., Nicolae Lerma, A., Desmazes, F., Perugini, E., Palmsten, M.L., Chickadel, C., 2021a. Sea state from single optical images: a methodology to derive wind-generated ocean waves from cameras, drones and satellites. Remote Sens. 13 https://doi.org/10.3390/rs13040679.

Almar, R., Bergsma, E.W.J., Thoumyre, G., Baba, M.W., Cesbron, G., Daly, C., Garlan, T., Lifermann, A., 2021b. Global satellite-based coastal bathymetry from waves. Remote Sens. 13, 4628. URL.

Anthony, E.J., 2004. The turtle bank, sherbro bay, west africa: estuarine-modified inner shelf shoal?. In: Proceedings of Marine Sandwave and River Dune Dynamics, Enschede, the Netherlands, p. 8 pp.

Anthony, E., Almar, R., Aagaard, T., 2016. Recent shoreline changes in the Volta river delta, west africa: the roles of natural processes and human impacts. Afr. J. Aquat. Sci. 41, 81–87. https://doi.org/10.2989/16085914.2015.1115751.

Anthony, E., Almar, R., Besset, M., Reyns, J., Laibi, R., Ranasinghe, R., Abessolo Ondoa, G., Vacchi, M., 2019. Response of the bight of Benin (gulf of guinea, west africa) coastline to anthropogenic and natural forcing, part 2: sources and patterns of sediment supply, sediment cells, and recent shoreline change. Cont. Shelf Res. 173, 93–103.

Baba, W.M., Thoumyre, G., Bergsma, E.W.J., Daly, C.J., Almar, R., 2021. Deriving Large-Scale Coastal Bathymetry from Sentinel-2 Images Using an High-Performance Cluster: A Case Study Covering North africa's Coastal Zone.

Banks, A.C., Mélin, F., 2015. An assessment of cloud masking schemes for satellite ocean colour data of marine optical extremes. Int. J. Remote Sens. 36, 797–821.

Becker, J., Sandwell, D., Smith, W.H.F., Braud, J., Binder, B., Depner, J., Fabre, D., Factor, J., Ingalls, S., Kim, S.H., Ladner, R., Marks, K., Nelson, S., Pharaoh, A., Trimmer, R., von Rosenberg, J., Wallace, G., Weatherall, P., 2009. Global bathymetry and elevation data at 30 arc seconds resolution: Srtm30_plus. Mar. Geod. 32, 355–371. https://doi.org/10.1080/01490410903297766.

Benveniste, J., Cazenave, A., Vignudelli, S., Fenoglio-Marc, L., Shah, R., Almar, R., Andersen, O., Birol, F., Bonnefond, P., Bouffard, J., Calafat, F., Cardellach, E., Cipollini, P., Le Cozannet, G., Dufau, C., Fernandes, M.J., Frappart, F., Garrison, J., Gommenginger, C., Han, G., Høyer, J.L., Kourafalou, V., Leuliette, E., Li, Z., Loisel, H., Madsen, K.S., Marcos, M., Melet, A., Meyssignac, B., Pascual, A., Passaro, M., Ribó, S., Scharroo, R., Song, Y.T., Speich, S., Wilkin, J., Woodworth, P., Wöppelmann, G., 2019. Requirements for a coastal hazards observing system. Front. Mar. Sci. 6, 348. https://doi.org/10.3389/fmars.2019.00348.

Bergsma, E.W.J., Almar, R., 2020. Coastal coverage of esa' sentinel 2 mission. Adv. Space Res. 65, 2636–2644. https://doi.org/10.1016/j.asr.2020.03.001.

Bergsma, E.W.J., Almar, R., Maisongrande, P., 2019a. Radon-augmentation of sentinel-ii imagery to enhance resolution and visibility of (nearshore) ocean-wave patterns, in. In: Proceedings of the International Geoscience and Remote Sensing Symposium (IGARSS). IEEE, Yokohama, Japan, pp. 7944–7947. https://doi.org/10.1109/IGARSS.2019.8898181.

Bergsma, E.W.J., Almar, R., Maisongrande, P., 2019b. Radon-augmented sentinel-2 satellite imagery to derive wave-patterns and regional bathymetry. Remote Sens. 11 https://doi.org/10.3390/rs11161918, 16 pp.

Bergsma, E.W.J., Almar, R., Rolland, A., Binet, R., Brodie, K.L., Bak, A.S., 2021. Coastal morphology from space: a showcase of monitoring the topography-bathymetry continuum. Remote Sens. Environ. 261, 112469. https://doi.org/10.1016/j.rse.2021.112469.

Bergsma, E.W., Almar, R., Anthony, E.J., Garlan, T., Kestenare, E., 2022. Wave variability along the world's continental shelves and coasts: Monitoring opportunities from satellite Earth observation. Adv. Space Res. 69 (9), 3236–3244. https://doi.org/10.1016/j.asr.2022.02.047.

Bian, X., Shao, Y., Zhang, C., Xie, C., Tian, W., 2020. The feasibility of assessing swell-based bathymetry using sar imagery from orbiting satellites. ISPRS J. Photogramm. Remote Sens. 168, 124–130. URL. https://www.sciencedirect.com/science/article/pii/S0924271620302148. https://doi.org/10.1016/j.isprsjprs.2020.08.006.

Caballero, I., Stumpf, R.P., 2019. Retrieval of nearshore bathymetry from sentinel-2a and 2b satellites in south florida coastal waters. Estuar. Coast. Shelf Sci. 226, 106277. URL. https://www.sciencedirect.com/science/article/pii/S0272771418309983. https://doi.org/10.1016/j.ecss.2019.106277.

Carrere, L., Lyard, F.H., Cancet, M., Guillot, A., 2016. Finite element solution fes2014, a new tidal model – validation results and perspectives for improvements. In: ESA Living Planet Conference (2016).

Cesbron, G., Melet, A., Almar, R., Lifermann, A., Tullot, D., Crosnier, L., 2021. Pan-European satellite-derived coastal bathymetry—review, user needs and future services. Front. Mar. Sci. 8, 1591. https://doi.org/10.3389/fmars.2021.740830.

Chénier, R., Faucher, M.A., Ahola, R., 2018. Satellite-derived bathymetry for improving Canadian hydrographic service charts. Int. J. Geo-Inform. 7, 15 pp.

Copernicus Climate Change Service (C3S), 2017. ERA5: Fifth generation of ECMWF atmospheric reanalyses of the global climate. Copernicus Climate Change Service Climate Data Store (CDS). URL: https://cds.climate.copernicus.eu/cdsapp#!/home. accessed: 2020-01-24.

Copernicus Climate Change Service, C, 2017. Era5: Fifth Generation of ecmwf Atmospheric Reanalyses of the Global Climate. https://cds.climate.copernicus.eu/cdsapp#!/home. Accessed: 2020-01-24.

Copernicus Data Access Portal, 2020. Sentinel-2 msi level-1c Cloud Masks. URL: https://sentinel.esa.int/web/sentinel/technical-guides/sentinel-2-msi/level-1c/cloud-masks. accessed: 2020-02-26.

Dada, O.A., Li, G., Qiao, L., Ding, D., Ma, Y., Xu, J., 2016. Seasonal shoreline behaviours along the arcuate Niger delta coast: complex interaction between fluvial and marine processes. Cont. Shelf Res. 122, 51–67. https://doi.org/10.1016/j.csr.2016.03.002.

Danilo, C., Melgani, F., 2016. Wave period and coastal bathymetry using wave propagation on optical images. IEEE Trans. Geosci. Remote Sens. 54, 6307–6319.

Dee, D.P., Uppala, S.M., Simmons, A.J., Berrisford, P., Poli, P., Kobayashi, S., Andrae, U., Balmaseda, M.A., Balsamo, G., Bauer, P., Bechtold, P., Beljaars, A.C.M., van de Berg, L., Bidlot, J., Bormann, N., Delsol, C., Dragani, R., Fuentes, M., Geer, A.J., Haimberger, L., Healy, S.B., Hersbach, H., Hólm, E.V., Isaksen, L., Kållberg, P., Köhler, M., Matricardi, M., McNally, A.P., Monge-Sanz, B.M., Morcrette, J.J., Park, B.K., Peubey, C., de Rosnay, P., Tavolato, C., Thépaut, J.N., Vitart, F., 2011. The era-interim reanalysis: configuration and performance of the data assimilation system. Q. J. R. Meteorol. Soc. 137, 553–597. https://doi.org/10.1002/qj.828.

GEBCO Compilation Group, . Gebco 2019 Grid. URL. https://www.gebco.net/data_and_products/gridded_bathymetry_data/. https://doi.org/10.5285/a29c5465-b138-234d-e053-6c86abc040b9. accessed: 2019-11-29.

Giardino, A., Schrijvershof, R., Nederhoff, C., de Vroeg, H., Brière, C., Tonnon, P.K., Caires, S., Walstra, D., Sosa, J., van Verseveld, W., Schellekens, J., Sloff, C., 2018. A quantitative assessment of human interventions and climate change on the west african sediment budget. Ocean Coast. Manag. 156, 249–265. https://doi.org/10.1016/j.ocecoaman.2017.11.008.

Hodúl, M., Bird, S., Knudby, A., Chénier, R., 2018. Satellite derived photogrammetric bathymetry. ISPRS J. Photogramm. Remote Sens. 142, 268–277. https://doi.org/10.1016/j.isprsjprs.2018.06.015.

Lamarche, C., Santoro, M., Bontemps, S., d'Andrimont, R., Radoux, J., Giustarini, L., Brockmann, C., Wevers, J., Defourny, P., Arino, O., 2017. Compilation and validation of sar and optical data products for a complete and global map of inland/ocean water tailored to the climate modeling community. Remote Sens. 9, 20 pp.

Lee, Z., Hu, C., Casey, B., Shang, S., Dierssen, H., Arnone, R., 2010. Global shallow-water from satellite ocean color data. Eos 91, 429–430.

Lyzenga, D.R., Malinas, N.P., Tanis, F.J., 2006. Multispectral bathymetry using a simple physically based algorithm. IEEE Trans. Geosci. Remote Sens. 44, 2251–2259. https://doi.org/10.1109/TGRS.2006.872909.

McMaster, R., Lachance, T.P., Ashraf, A., 1970. Continental shelf geomorphic features off portuguese guinea, guinea, and Sierra Leone (west africa). Mar. Geol. 9, 203–213.

Melet, A., Teatini, P., Le Cozannet, G., Jamet, C., Conversi, A., Benveniste, J., Almar, R., 2020. Earth observations for monitoring marine coastal hazards and their drivers. Surv. Geophys. https://doi.org/10.1007/s10712-020-09594-5 [Early access], p. [46 p.].

Ndour, A., Laïbi, R.A., Sadio, M., Degbe, Cossi G.E., Diaw, A.T., Oyédé, L.M., Anthony, E.J., Dussouillez, P., Sambou, H., Dièye, E.H.B., 2018. Management strategies for coastal erosion problems in west africa: analysis, issues, and constraints drawn from the examples of Senegal and Benin. Ocean Coast. Manag. 156, 92–106.

Pacheco, A., Horta, J., Loureiro, C., Ferreira, O., 2015. Retrieval of nearshore bathymetry from landsat 8 images: a tool for coastal monitoring in shallow waters. Remote Sens. Environ. 159, 102–116.

Parrish, C.E., Magruder, L.A., Neuenschwander, A.L., Forfinski-Sarkozi, N., Alonzo, M., Jasinski, M., 2019. Validation of icesat-2 atlas bathymetry and analysis of atlas's bathymetric mapping performance. Remote Sens. 11 https://doi.org/10.3390/rs11141634.

Poupardin, A., Idier, D., de Michele, M., Raucoules, D., 2016. Water depth inversion from a single spot-5 dataset. IEEE Trans. Geosci. Remote Sens. 54, 2329–2342.

Salameh, E., Frappart, F., Almar, R., Baptista, P., Heygster, G., Lubac, B., Raucoules, D., Almeida, L.P., Bergsma, E.W.J., Capo, S., De Michele, M., Idier, D., Li, Z., Marieu, V., Poupardin, A., Silva, P.A., Turki, I., Laignel, B., 2019. Monitoring beach topography and nearshore bathymetry using spaceborne remote sensing: a review. Remote Sens. 11 https://doi.org/10.3390/rs11192212, 32 pp.

Saylam, K., Hupp, J.R., Averett, A.R., Gutelius, W.F., Gelhar, B.W., 2018. Airborne lidar bathymetry: assessing quality assurance and quality control methods with leica chiroptera examples. Int. J. Remote Sens. 39, 2518–2542. https://doi.org/10.1080/01431161.2018.1430916.

Smith, W.H.F., Sandwell, D.T., 1997. Global sea floor topography from satellite altimetry and ship depth soundings. Science 277, 1956–1962.

Smith, W.H., Sandwell, D.T., 2004. Conventional bathymetry, bathymetry from space, and geodetic altimetry. Oceanography 17, 8–23.

Stewart, C., Renga, D.A., Gaffney, P.V., Schiavon, P.G., 2016. Sentinel-1 bathymetry for north sea palaeolandscape analysis. Int. J. Remote Sens. 37, 471–491. https://doi.org/10.1080/01431161.2015.1129563.

Stumpf, R.P., Holderied, K., Sinclair, M., 2003. Determination of water depth with high-resolution satellite imagery over variable bottom types. Limnol. Oceanogr. 48, 547–556.

Thomas, N., Pertiwi, A.P., Traganos, D., Lagomasino, D., Poursanidis, D., Moreno, S., Fatoyinbo, L., 2021. Space-borne cloud-native satellite-derived bathymetry (sdb) models using icesat-2 and sentinel-2. Geophys. Res. Lett. 48 https://doi.org/10.1029/2020GL092170 e2020GL092170. URL.

Traganos, D., Poursanidis, D., Aggarwal, B., Chrysoulakis, N., Reinartz, P., 2018. Estimating satellite-derived bathymetry (sdb) with the google earth engine and sentinel-2. Remote Sens. 10, 18 pp.